Alexandria Engineering Journal (2015) 54, 941–953

HOSTED BY
ELSEVIER

Alexandria University

Alexandria Engineering Journal

www.elsevier.com/locate/aej
www.sciencedirect.com

REVIEW

MHD boundary layer slip flow and radiative nonlinear heat transfer over a flat plate with variable fluid properties and thermophoresis

S.K. Parida [a,*], S. Panda [b], B.R. Rout [c]

[a] *Department of Mathematics, ITER, S'O'A University, Bhubaneswar, 751030 Odisha, India*
[b] *Department of Mathematics, NIT Calicut, NIT(P.O), 673601 Kerala, India*
[c] *Department of Mathematics, Krupajal Engineering College, Bhubaneswar, 751002 Odisha, India*

Received 30 April 2015; revised 17 August 2015; accepted 19 August 2015
Available online 26 September 2015

KEYWORDS

Thermophoresis;
Variable thermal conductivity;
Variable viscosity;
Non-linear radiation;
Slip flow

Abstract This work considers the two-dimensional steady MHD boundary layer flow of heat and mass transfer over a flat plate with partial slip at the surface subjected to the convective heat flux. The particular attraction lies in searching the effects of variable viscosity and variable thermal diffusivity on the behavior of the flow. In addition, non-linear thermal radiation effects and thermophoresis are taken into account. The governing nonlinear partial differential equations for the flow, heat and mass transfer are transformed into a set of coupled nonlinear ordinary differential equations by using similarity variable, which are solved numerically by applying Runge–Kutta fourth–fifth order integration scheme in association with quasilinear shooting technique. The novel results for the dimensionless velocity, temperature, concentration and ambient Prandtl number within the boundary layer are displayed graphically for various parameters that characterize the flow. The local skin friction, Nusselt number and Sherwood number are shown graphically. The numerical results obtained for the particular case are fairly in good agreement with the result of Rahman [6].

Contents

* Corresponding author.
E-mail address: sparidamath2007@rediffmail.com (S.K. Parida).
Peer review under responsibility of Faculty of Engineering, Alexandria University.

http://dx.doi.org/10.1016/j.aej.2015.08.007
1110-0168

Nomenclature

$\mathbf{v}$	velocity (m s^{-1})
T	temperature (K)
T_w	temperature at the surface of the plate (K)
t_p	thermophoretic coefficient
C	concentration (mol m^{-3})
C_∞	concentration of the ambient fluid (mol m^{-3})
$\mathbf{B}$	magnetic field (N m^{-1} A^{-1})
p	pressure (N m^{-2})
c_p	specific heat of the fluid at constant pressure (J kg^{-1} K^{-1})
$\mathbf{q_c}$	heat flux (W m^{-2})
q'''	non-uniform heat generated or absorbed (kg m^{-1} s^{-3})
q_w	surface heat flux (W m^{-2})
x, y	distance along and normal to the plate (m)
k	thermal conductivity (W m^{-1} K^{-1})
k_∞	thermal conductivity at ambient temperature (W m^{-1} K^{-1})
h	heat transfer coefficient (W m^{-2} K^{-1})
Ha	Hartmann number
Gr	Grashof number
R	radiation parameter
Pr	variable Prandtl number
Re_x	local Reynolds number
Sh_x	local Sherwood number
$\mathbf{f}$	Lorentz force (N m^{-3})
T_∞	temperature of the ambient fluid (K)
L	slip length (m)
T_f	reference temperature (K)
U_∞	free stream velocity (m s^{-1})
C_w	concentration of the fluid at the plate (mol m^{-3})
$\mathbf{g}$	acceleration due to gravity (ms^{-2})
Q_s, Q_t	constants
$\mathbf{E}$	electric field (kg m s^{-3} A^{-1})
$\mathbf{J}$	current density (A m^{-2})
A	constant
$\mathbf{q}_r$	radiative heat flux (W m^{-2})
D	mass diffusivity (m^2 s^{-1})
m_w	surface mass flux (mol m^{-2} s^{-1})
a	surface convection parameter
a_1, a_2	constants
k_s	mean absorption coefficient (m^{-1})
$\mathbf{V}_T$	thermophoretic velocity (m s^{-1})
b, T_r	constants
C_f	skin friction coefficient
Nu_x	local Nusselt number
Gc	solutal Grashof number
Sc	Schmidt number
Pr_∞	ambient Prandtl number
$Kn_{x,L}$	local Knudsen number
Nc	concentration difference parameter

Greek symbols

ρ	density (kg m^{-3})
μ_∞	dynamic viscosity at ambient temperature (N m^{-2})
ν_∞	kinematic viscosity far away from the sheet (m^2 s^{-1})
σ_0	electric conductivity (s^3 A^2 m^{-3} kg^{-1})
β	coefficient of thermal expansion (K^{-1})
θ_r	variable viscosity parameter
ϵ	variable thermal conductivity parameter
σ^*	Boltzmann constant (W m^{-2} K^{-4})
γ	constant associated with thermal property of the fluid
β^*	expansion coefficient with concentration (concentration^{-1})
μ	dynamic viscosity (N s m^{-2})
λ	plate surface concentration exponent
ν	kinematic viscosity (m^2 s^{-1})
ψ	stream function
ϕ	non-dimensional concentration
η	non-dimensional space variable
θ	non-dimensional temperature variable
θ_w	temperature ratio parameter
τ	thermophoretic parameter
δ	slip parameter
α	thermal property of the fluid
τ_w	viscous stress at the surface of the plate (N m^{-2})

Operator

∇	nabla operator

1. Introduction

The wide applications of laminar boundary layer flows of heat and mass transfer over a flat surface in different areas of science and engineering have attracted the attention of many researchers. Specific examples of such flows occur in the design of cooling systems for electronic devices, in the field of geothermal reservoirs, heat exchangers, cooling of nuclear reactor, etc. The first concept of similarity solution formulated by Blasius [1] for the boundary layer flow of a Newtonian fluid over a flat surface forms the basis for several subsequent studies. Later it has been extended by many researchers (e.g., Fang

[2], Makinde [3], Cortell [4], Shu et al. [5]) to explore the similar solutions for thermal boundary layer flows over a flat plate under different flow configurations and boundary conditions. Recent studies include the work of Rahman [6]. The author studied the hydromagnetic convective flow of electrically conducting fluid over a flat plate with partial slip and convective heat flux conditions at the boundary.

The similarity solution for the thermal boundary layer flow of Newtonian fluid with convective surface heat flux conditions has been developed by Aziz [7]. The problem has been revisited later on several times with the inclusion of physics or more complex rheology. Bataller [8], for example, extended Aziz's contribution by analyzing Sakiadis flows with thermal radiation effects, while Ishak [9] considered the permeable flat surface. Yao et al. [10] concentrated on the heat transfer flow of a generalized stretching/shrinking wall with convective boundary condition. Similar analyses have been performed by Uddin et al. [11–14] for boundary layer flow of a nanofluid using scaling group of transformation. A common feature of the literature cited above is that it assumed the constant fluid properties such as constant viscosity and thermal conductivity. Most of the existing analytical studies for this type of problems have emphasized on constant physical properties of the ambient fluid. The variation of viscosity in thermal boundary layer is quite useful and significant in experimental studies such as glass fiber production, paper production, wire drawing, and drawing of plastic films. Recognizing the restriction of constant fluid properties assumptions, Prasad et al. [15] extended the formulation to account for variable thermal conductivity in a non-isothermal stretching sheet through power law fluids. Recently this work has been extended to include the combined effects of thermal buoyancy and variable thermal conductivity on magneto hydrodynamic flow (Abel et al. [16]), and it is reported that variable thermal conductivity substantially influences the shear stress enhancement. Many researchers (e.g., Elbarbary et al. [17], Seddeek et al. [18], Rahman et al. [19]) have studied the effect of variable fluid properties of MHD fluid flows in the last few years.

The no-slip boundary condition is extensively applied for flows involving Newtonian and non-Newtonian fluid past solid boundary. But, in many instances the no-slip boundary condition exhibits inaccurate results, like the incapability of the no-slip condition at the solid–fluid interface for the flow of fluids in a microelectromechanical system is no longer applicable. It has also been found that there is a large class of polymeric materials slip or stick–slip on solid boundaries (Rao et al. [20]). Thus, it is a well recognized subject as evident from the literature (Yoshimura et al. [21], Hasimoto [22], Martin et al. [23–25], Vedantam [26], Fang et al. [27], Andersson [28], Wang [29], Aziz [30], Sahoo [31]).

The study of radiation on the various types of flows is quite complicated. In the recent years, many authors (Seddeek et al. [32], Pal et al. [33], Mahdy [34], Rout et al. [35], Balla et al. [36]) have studied the effects of radiation on the boundary layer of radiating fluid in various problems. A more recent study (Rahman et al. [37,38]) has predicted that the Prandtl number must be treated as a variable rather than a constant in characterizing the variable viscosity and thermal conductivity in a thermal boundary layer flow. The effect of non-linear radiation has been considered (Cortell [39]) due to high temperature difference for the boundary layer flow over a stretching sheet.

The uneven temperature distribution on the flat surfaces creates temperature gradient and has effect on the movement of molecules. As a result the molecules in the hot region move faster than the molecules in the cold region. This leads to a movement of particles in the direction opposite to the temperature gradient, i.e. from warmer areas to cooler areas. The physics behind this phenomenon are known as thermophoresis. Thermophoresis is of practical importance in a variety of industrial and engineering applications including aerosol collection (thermal precipitators), nuclear reactor safety, corrosion of heat exchangers, and microcontamination control. Goldsmith et al. [40] first studied the thermophoretic transport involved in a simple one-dimensional flow for the measurement of the thermophoretic velocity. Later the variable suction and thermophoresis effects on steady MHD combined free-forced convective heat and mass transfer flow over a semi-infinite permeable inclined plate including thermal radiation were discussed by Alam et al. [41]. Recently El-Sayed et al. [42] have focused on the effectiveness of variable viscosity and variable thermal diffusivity on steady MHD heat and mass transfer flow over a semi-infinite porous inclined plate in the presence of thermal radiation and thermophoresis. The effects of variable fluid properties on the thermophoretic MHD slip flow over a permeable surface with linear radiation have been recently studied by Das et al. [43].

Effects of heat transfer on the flow dynamics of hydromagnetic thermal boundary layer flow of a viscous fluid over a flat plate with variable fluid properties in the presence of partial slip with the convective heat flux at the surface have been studied recently by Rahman [6]. But, so far no attempt has been made to analyze the effects of thermophoresis particle deposition on convective heat and mass transfer past a flat heated plate with variable fluid properties and non-linear radiation in the presence of slip and convective boundary conditions, and hence we have considered the problem of this kind. The mass deposition variation on the surface is taking into our problem to know the effects of thermophoresis. Therefore, the objective of the present paper was to investigate the effects of variable viscosity, and variable thermal diffusivity on steady mass and non-linear radiative heat transfer process in a two-dimensional MHD convective flow over a flat plate with partial slip at the surface subjected to the convective surface heat flux with thermophoresis. Thus, the main purpose of the analysis was to investigate how the flow field, temperature and concentration fields vary within the boundary layer for a hydromagnetic slip flow when both the thermal conductivity and viscosity are temperature dependent subjected to thermophoresis and non-linear radiative effects. The local similarity equations are derived and solved numerically and the graphs and tables are presented to illustrate and discuss important hydrodynamic and thermal features of the flow.

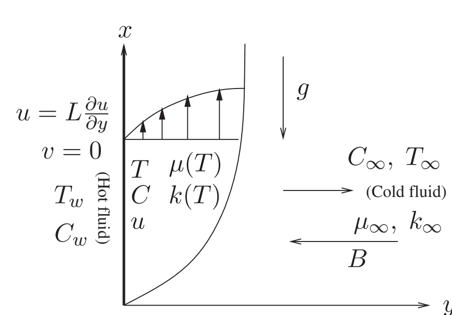

Figure 1 Sketch of flow geometry.

2. The physical model and problem formulation

We consider a two dimensional MHD flow of a viscous incompressible, heat generating and absorbing, electrically conducting fluid moving over the surface of a semi-infinite impermeable flat plate with a stream of cold fluid at uniform velocity U_∞, temperature T_∞ and concentration C_∞ in the presence of radiation. The viscosity and thermal conductivity of the fluid are assumed to be functions of temperature. The thermophoresis effect is considered for the understanding of the mass deposition variation on the surface. It is further assumed that the lower surface of the plate is being heated by convection from a hot fluid at temperature T_w that provides a heat transfer coefficient h_f. The concentration of the fluid near the plate is denoted by C_w. Here the x-axis is taken along the direction of plate and y-axis is normal to it, as shown in Fig. 1.

A magnetic field is applied in the direction perpendicular to the plate with varying strength as a function of x. Neglecting the viscous dissipation and Joule heating, the governing equations for a steady two-dimensional flow can be written as follows:

Continuity equation

$$\nabla \cdot \mathbf{v} = 0 \tag{1}$$

Momentum equation

$$\rho(\mathbf{v}\cdot\nabla)\mathbf{v} = -\nabla p + \nabla\cdot(\mu(T)\nabla\mathbf{v}) + \rho\mathbf{g}(\beta(T-T_\infty) + \beta^*(C-C_\infty)) + \mathbf{f} \tag{2}$$

Temperature equation

$$\rho c_p(\mathbf{v}\cdot\nabla)T = -\nabla\cdot(\mathbf{q}_c + \mathbf{q}_r) + q''' \tag{3}$$

Concentration equation

$$(\mathbf{v}\cdot\nabla)C = D\nabla\cdot(\nabla C) - \nabla\cdot(\mathbf{v}_T C) \tag{4}$$

The symbols $\mathbf{v} = (u, v), \rho, p, T$ and C denote the fluid velocity, the constant density, the pressure, the temperature and the concentration. Here c_p and $\mathbf{g}$ are the constant heat capacity and acceleration due to gravity, β is the coefficient of thermal expansion, β^* is the coefficient of expansion with concentration, μ is the variable viscosity, $\mathbf{f}$ is the source term due to imposed magnetic field, q''' is the non-uniform heat generated (>0) or absorbed (<0) per unit volume and $\mathbf{v}_T$ is the thermophoretic velocity. Here $\mathbf{q}_c$ and $\mathbf{q}_r$ are the conduction and radiation flux vectors, respectively. The symbol ∇ denotes the gradient operator.

The external force $\mathbf{f}$ may be written as follows:

$$\mathbf{f} = \mathbf{J}\times\mathbf{B}, \tag{5}$$

where $\mathbf{J} = \sigma_0(\mathbf{E} + \mathbf{v}\times\mathbf{B})$ is the current density and $\mathbf{B} = (0, B(x))$ is the transverse uniform magnetic field applied to the fluid layer. The symbols σ_0 and $\mathbf{E}$ are the electric conductivity and the electric field, respectively. The external electric field is assumed to be zero and under the condition that magnetic Reynolds number is small the induced magnetic field is negligible compared with the applied field. Accordingly, the Hall effect is neglected.

The conduction heat flux is given by,

$$\mathbf{q}_c = -k(T)\nabla T, \tag{6}$$

where k is the variable heat conductivity. Expression for radiative heat flux $\mathbf{q}_r$ can be obtained using Rosseland approximation (Sparrow et al. [45])

$$\mathbf{q}_r = -\frac{4\sigma^*}{3k_s}\nabla T^4, \tag{7}$$

where k_s is the Rosseland mean absorption coefficient and σ^* is the Stefan–Boltzmann constant. Assuming the high temperature difference (Cortell [39]), Eq. (7) can be written as

$$\mathbf{q}_r = -\frac{16\sigma^*}{3k_s}T^3\nabla T. \tag{8}$$

In our present study, we have considered the effect of thermophoresis and the thermophoretic velocity $\mathbf{v}_T$ which appears in Eq. (13), can be written as (Talbot et al. [46])

$$\mathbf{v}_T = -\frac{\mu(T)t_p}{\rho T_f}\nabla T, \tag{9}$$

where the term $t_p\mu(T)/\rho$ represents the thermophoretic diffusivity, with T_f some reference temperature and t_p the thermophoretic coefficient which ranges in value from 0.2 to 1.2 as indicated by Batchelor et al. [47]. In the boundary layer flow the thermophoretic velocity component which is normal to the surface is of importance as the temperature gradient in the y-direction is much larger than that in the x-direction.

Within the framework of the above noted assumptions, the basic governing boundary layer equations for mixed convection flow under Boussinesq approximation can be written in the simplified form as follows:

$$\frac{\partial u}{\partial x} + \frac{\partial v}{\partial y} = 0 \tag{10}$$

$$u\frac{\partial u}{\partial x} + v\frac{\partial u}{\partial y} = \frac{1}{\rho}\frac{\partial}{\partial y}\left(\mu(T)\frac{\partial u}{\partial y}\right) + g\beta(T-T_\infty) + g\beta^*(C-C_\infty) - \frac{\sigma_0}{\rho}B^2(x)(u-U_\infty) \tag{11}$$

$$\rho c_p\left(u\frac{\partial T}{\partial x} + v\frac{\partial T}{\partial y}\right) = \frac{\partial}{\partial y}\left(\left(k(T) + \frac{16\sigma^*}{3k_s}T^3\right)\frac{\partial T}{\partial y}\right) + q''' \tag{12}$$

$$u\frac{\partial C}{\partial x} + v\frac{\partial C}{\partial y} = D\frac{\partial^2 C}{\partial y^2} + \frac{t_p}{\rho T_f}\frac{\partial}{\partial y}\left(\mu(T)C\frac{\partial T}{\partial y}\right) \tag{13}$$

The boundary conditions relevant to the present problem are as follows:

$$\begin{aligned} u(x,0) &= L\frac{\partial u}{\partial y}(x,0),\ v(x,0) = 0,\ -k(T)\frac{\partial T}{\partial y}(x,0) \\ &= h_f(T_w - T(x,0)), C_w(x,0) = Ax^\lambda + C_\infty, \\ u(x,\infty) &= U_\infty,\ T(x,\infty) = T_\infty,\ C(x,\infty) = C_\infty, \end{aligned} \tag{14}$$

where L is the slip length, $A(>0)$ is constant, λ is the plate surface concentration exponent and the subscripts w and ∞ refer to the wall and boundary layer edge respectively.

It is known that the fluid properties may change with temperature and to accurately predict the flow and heat transfer rates, it is necessary to take into account this variation of viscosity and thermal diffusivity. Thus in order to predict the flow and heat transfer rates accurately, for fluid we suggest a viscosity dependence on temperature T of the following form:

$$\mu(T) = \frac{\mu_\infty}{1+\gamma(T-T_\infty)}, \tag{15}$$

where constant γ is associated with the thermal property of fluid. Eq. (15) can also be written as,

$$\mu(T) = \frac{1}{b(T-T_r)}, \tag{16}$$

where $b = \gamma/\mu_\infty$ and $T_r = T_\infty - 1/\gamma$. Here b and T_r are constants, whose values depend on the thermal property of the fluid γ. It is found that $b > 0$ for liquids and $b < 0$ for gases.

The thermal conductivity is a linear function of temperature (Chiam [44]) which can be defined as

$$k(T) = k_\infty\left(1+\epsilon\left(\frac{T-T_\infty}{T_w-T_\infty}\right)\right), \tag{17}$$

where ϵ is the variable thermal conductivity parameter and k_∞ is the thermal conductivity of the fluid far away from the plate.

The internal heat generation or absorption term q''' is chosen as (Das et al. [43])

$$q''' = \frac{k_\infty U_\infty}{x\nu_\infty}\left(Q_s(T_w-T_\infty)e^{-\alpha^* y} + Q_t(T-T_\infty)\right), \tag{18}$$

where Q_s and Q_t are the non-dimensional parameters of space-dependent and temperature-dependent heat source/sink. The symbol α^* is used for the thermal property of the fluid. For the internal heat generation both the parameters are positive and when both the parameters are negative then it corresponds to internal heat absorption.

For a similarity solution of Eqs. (10)–(13), we introduce the stream function ψ as $(u, v) = (\partial\psi/\partial y, -\partial\psi/\partial x)$. Following Das et al. [43] and Rahman [6], the similarity variable η and similarity functions $f(\eta), \theta(\eta)$ and $\phi(\eta)$ are defined as,

$$\psi = \sqrt{\nu_\infty U_\infty x}\, f(\eta), \quad \theta(\eta) = \frac{T-T_\infty}{T_w-T_\infty},$$
$$\phi(\eta) = \frac{C-C_\infty}{C_w-C_\infty}, \quad \eta = y\sqrt{\frac{U_\infty}{\nu_\infty x}}, \tag{19}$$

where $\nu_\infty = \mu_\infty/\rho$ is the coefficient of kinematic viscosity far away from the plate and μ_∞ refers to the viscosity of the fluid far away from the sheet. The continuity equation holds for any f and η and the Eqs. (11)–(13) reduce to

$$\frac{\theta_r}{\theta_r-\theta}f''' + \frac{\theta_r}{(\theta_r-\theta)^2}f''\theta' + \frac{1}{2}f''f + Gr\theta + Gc\phi - Ha^2(f'-1) = 0 \tag{20}$$

$$(1+\epsilon\theta)\theta'' + \epsilon\theta'^2 + R\left(((\theta_w-1)\theta+1)^3\theta'\right)' + \frac{1}{2}Pr\left(1-\frac{\theta}{\theta_r}\right)(1+\epsilon\theta)f\theta' + Q_s e^{-\alpha\eta} + Q_t\theta = 0 \tag{21}$$

Table 1 Comparison values of Pr_∞ at the surface of the plate for various values of θ_r and δ.

θ_r	Rahman results [6]			Present results		
	$\delta = 0$	$\delta = 0.5$	$\delta = 5$	$\delta = 0$	$\delta = 0.5$	$\delta = 5$
−0.001	147.50	126.49	124.34	147.50	126.23	123.93
−0.010	29.82	26.30	25.50	29.80	26.29	25.49
−0.100	6.03	5.56	5.32	5.69	5.53	5.29
−1	1.86	1.80	1.74	1.83	1.78	1.73
−5	1.38	1.36	1.33	1.36	1.35	1.32
−100	1.26	1.25	1.23	1.25	1.24	1.22
−1000	1.25	1.24	1.23	1.24	1.23	1.22
$-\infty$	1.25	1.24	1.23	1.24	1.23	1.22

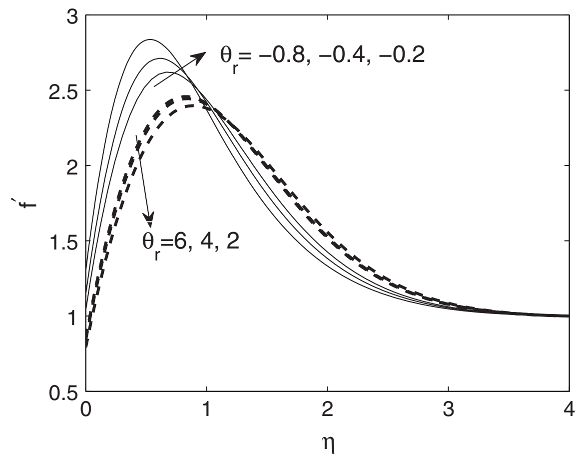

Figure 2 Velocity profiles for various values of variable viscosity parameter θ_r.

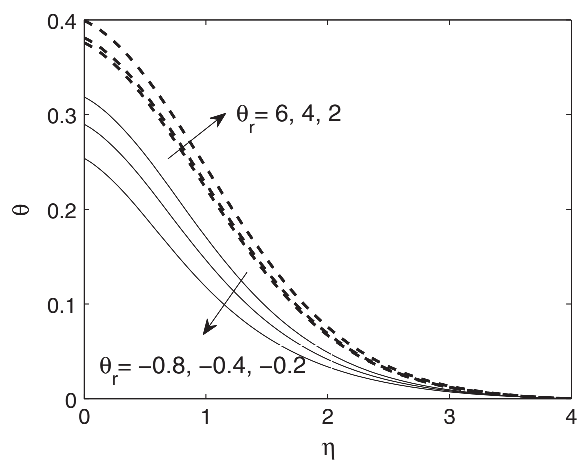

Figure 3 Temperature profiles for various values of variable viscosity parameter θ_r.

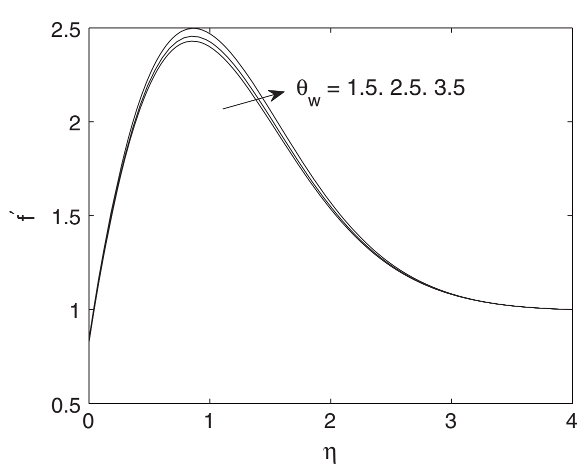

Figure 4 Velocity profiles for various values of temperature ratio parameter θ_w.

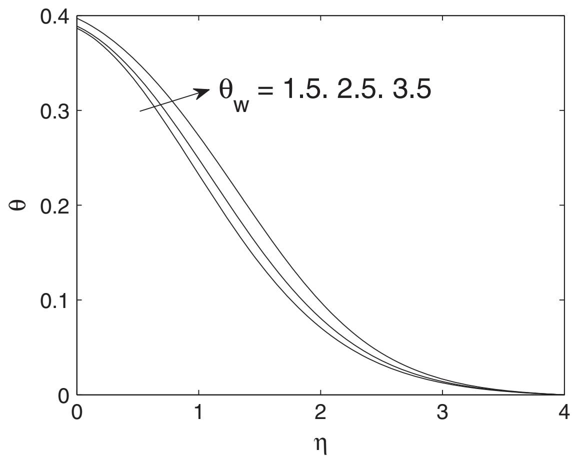

Figure 5 Temperature profiles for various values of temperature ratio parameter θ_w.

$$\phi'' + \frac{1}{2}Scf\phi' - \tau Sc\frac{\theta_r}{\theta_r - \theta}\left(\theta''\phi + \theta'\phi' + \frac{\phi(\theta')^2}{\theta_r - \theta} + Nc\left(\theta'' + \frac{(\theta')^2}{\theta_r - \theta}\right)\right) = 0. \quad (22)$$

with the boundary conditions

$$f(0) = 0, \quad f'(0) = \delta f''(0), \quad \theta'(0) = a\left(\frac{\theta(0) - 1}{1 + \epsilon\theta(0)}\right), \quad \phi(0) = 1,$$
$$f'(\infty) = 1, \quad \theta(\infty) = 0, \quad \phi(\infty) = 0, \quad (23)$$

where $\theta_r = (T_r - T_\infty)/(T_w - T_\infty) = -1/(\gamma(T_w - T_\infty))$ is the fluid viscosity parameter, $\theta_w = T_w/T_\infty$ is the temperature ratio parameter, $Ha = B_0\sqrt{\sigma_0/\rho U_\infty}$ is the magnetic parameter, $Gr = g\beta x(T_w - T_\infty)/U_\infty^2$ is the Grashof number, $Gc = g\beta^* x(C_w - C_\infty)/U_\infty^2$ is the solutal Grashof number, $R = 16\sigma^* T_\infty^3/3k_s k_\infty$ is the radiation parameter, $\alpha = \alpha^*\sqrt{v_\infty x/U_\infty}$ is the thermal property of the fluid, $Sc = v_\infty/D$ is the Schmidt number, $\tau = -t_p(T_w - T_\infty)/T_f$ is the thermophoretic parameter, $Nc = C_\infty/(C_w - C_\infty)$ is the concentration difference parameter and $a = (h_f/k_\infty)\sqrt{v_\infty x/U_\infty}$ is the surface convection parameter.

The non-dimensional slip parameter is defined in terms of local Knudsen number $(Kn_{x,L})$ and local Reynolds number (Re_x) i.e., $\delta = L\sqrt{U_\infty/xv_\infty} = Kn_{x,L}Re_x^{\frac{1}{2}}$, where $Kn_{x,L} = L/x$ and $Re_x = U_\infty x/v_\infty$.

The Prandtl number which can be defined by $Pr = \mu(T)c_p/k(T)$ is expressed in terms of Prandtl number at infinity $(\Pr_\infty = \mu_{\infty C_p}/k_\infty)$ by the following relation:

$$Pr = \frac{\theta_r Pr_\infty}{(\theta_r - \theta)(1 + \epsilon\theta)} \quad (24)$$

The relation Eq. (24) is valid due to variation of both viscosity and thermal conductivity across the boundary layer (see e.g., Rahman [6]).

In order to have similarity transformation it is assumed that the applied magnetic field $B(x)$ and convective heat transfer coefficient h_f are proportional to $x^{-1/2}$ and we can therefore assume (Aziz [7], Makinde [48], Rahman [6])

$$B(x) = B_0 x^{-1/2} \text{ and } h_f = h_{f_0} x^{-1/2}, \quad (25)$$

where B_0 and h_{f_0} are constants. Further, it is to be noted that the parameters Gr and Gc appearing in Eq. (20) are functions of x. Thus, to have similarity solution of the problem, we assume $\beta = a_1 x^{-1}$ and $\beta^* = a_2 x^{-1}$, where a_1, and a_2 are constants.

2.1. Skin friction, Nusselt number and Sherwood number

The parameters of engineering interest for the present problem are the local skin friction coefficient, local Nusselt number and the local Sherwood number which indicate physically wall shear stress, rate of heat transfer and rate of mass transfer, respectively.

The skin-friction coefficient is given by

$$C_f = \frac{\tau_w\sqrt{x}}{U_\infty^{3/2}\sqrt{\rho\mu_\infty}}, \quad (26)$$

where τ_w is the stress at the plate, i.e.

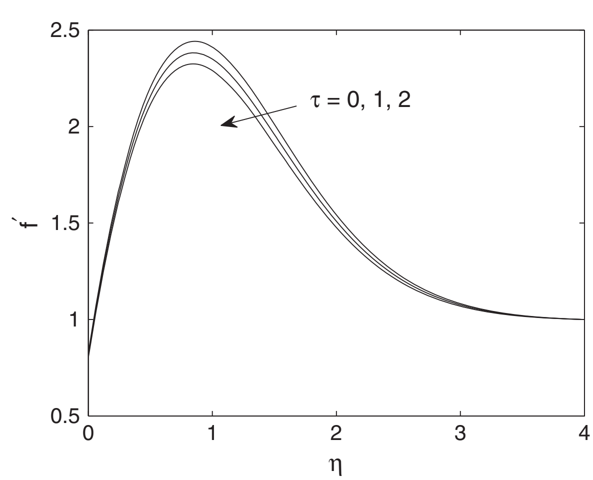

Figure 6 Velocity profiles for various values of thermophoretic parameter τ.

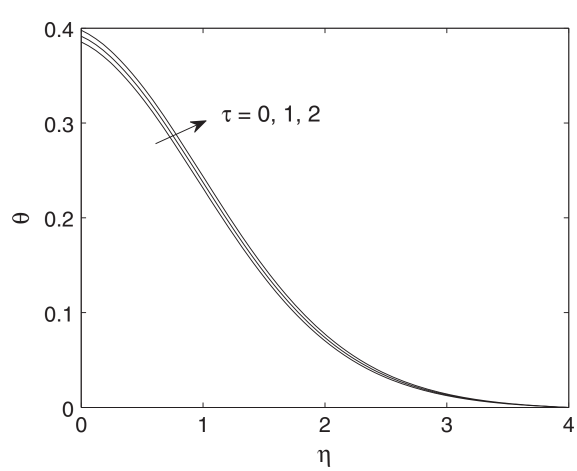

Figure 7 Temperature profiles for various values of thermophoretic parameter τ.

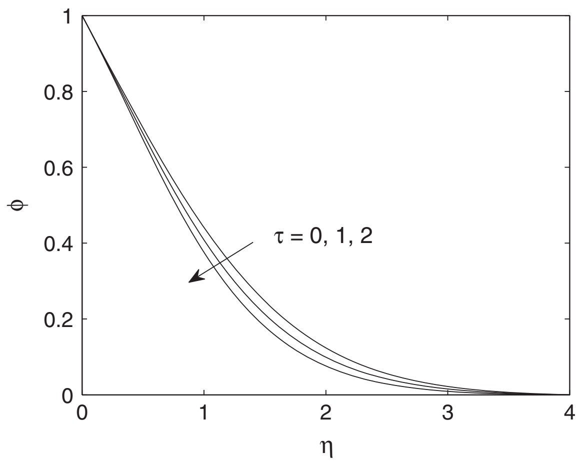

Figure 8 Concentration profiles for various values of thermophoretic parameter τ.

$$\tau_w = \mu(T)\frac{\partial u}{\partial y}|_{y=0} \tag{27}$$

Using the similarity variables Eq. (19), we get

$$C_f = \left(\frac{\theta_r}{(\theta_r - \theta(0))}\right) f''(0). \tag{28}$$

It is important to know the rate of heat transfer between the fluid and the plate and it is analyzed through non-dimensional Nusselt number and defined as

$$Nu_x = \frac{q_w\sqrt{\nu_\infty x}}{k_\infty(T_w - T_\infty)\sqrt{U_\infty}}, \tag{29}$$

where q_w is the surface heat flux, i.e.

$$q_w = -\left(\left(k(T) + \frac{16\sigma^*}{3k_s}T^3\right)\frac{\partial T}{\partial y}\right)_{y=0} \tag{30}$$

Using similarity variables defined in Eq. (19), we get

$$Nu_x = -(1 + \epsilon\theta(0) + R(1 + \theta(0)(\theta_w - 1))^3)\theta'(0) \tag{31}$$

The ratio of convective to diffusive mass transport can be analyzed through non-dimensional Sherwood number i.e.,

$$Sh_x = \frac{m_w}{D(C_w - C_\infty)}\sqrt{\frac{\nu_\infty x}{U_\infty}}, \tag{32}$$

where the mass flux m_w at the plate is defined as

$$m_w = -D\left(\frac{\partial C}{\partial y}\right)_{y=0} \tag{33}$$

Using non-dimensional relation, we get

$$Sh_x = -\phi'(0) \tag{34}$$

3. Results and discussion

3.1. Numerical procedure

The system of coupled non-linear differential Eqs. (20)–(22) with boundary conditions Eq. (23) are solved numerically. In order to solve the system of equations we first convert these equations into first order differential equations. Then the first order differential equations are solved using Runge–Kutta fourth–fifth order method in association with shooting technique. In the following section the simulation results of different variations of flow parameters are presented and discussed. In addition, for validating the accuracy of our numerical results, we have compared our results with the previous published data from Rahman [6] in Table 1.

3.2. Computational results for velocity, temperature and concentration profiles

The numerical results of non-dimensional velocity, temperature and concentration for various values of physical parameters are shown in Figs. 2–20. The parameters used for simulation are, unless otherwise stated: $\theta_r = 3, Gr = 5, Gc = 5, Ha = 0.5, R = 0.2, \theta_w = 1.5, Q_s = 0.3, Q_t = 0.2, Pr = 1.0, Sc = 0.6, \tau = 0.2, Nc = 0.2, \delta = 0.2$. $a = 0.1$, $\epsilon = 0.1$ and $\alpha = 1.0$.

Effects of variable viscosity parameter θ_r on velocity and temperature profiles are analyzed in Figs. 2 and 3, respectively.

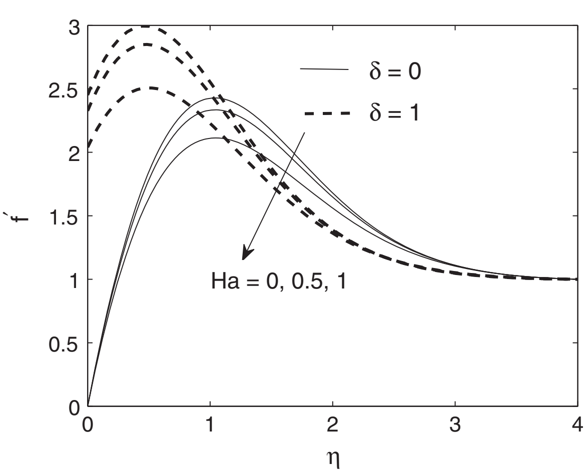

Figure 9 Velocity profiles for various values of magnetic parameter M at $\delta = 0$ and $\delta = 1$.

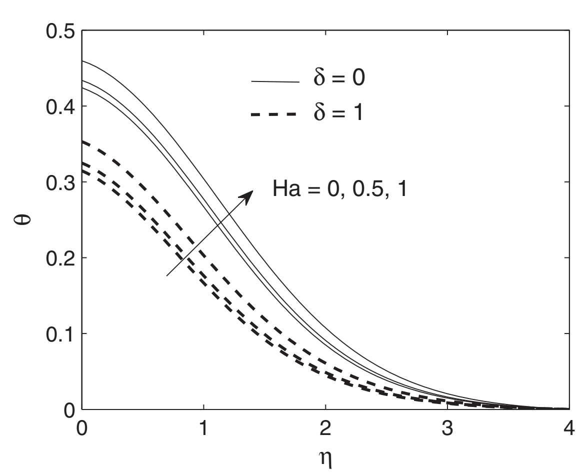

Figure 10 Temperature profiles for various values of magnetic parameter M at $\delta = 0$ and $\delta = 1$.

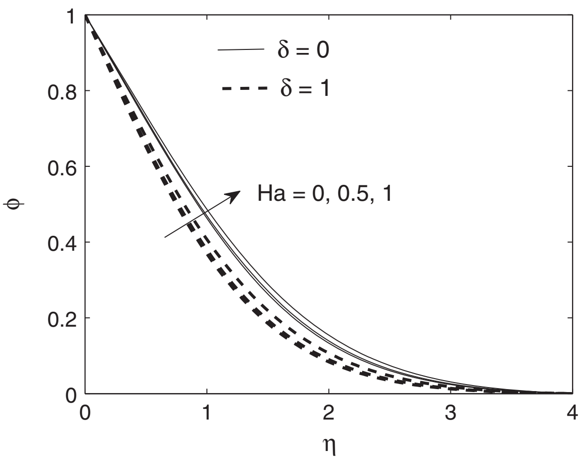

Figure 11 Concentration profiles for various values of magnetic parameter M at $\delta = 0$ and $\delta = 1$.

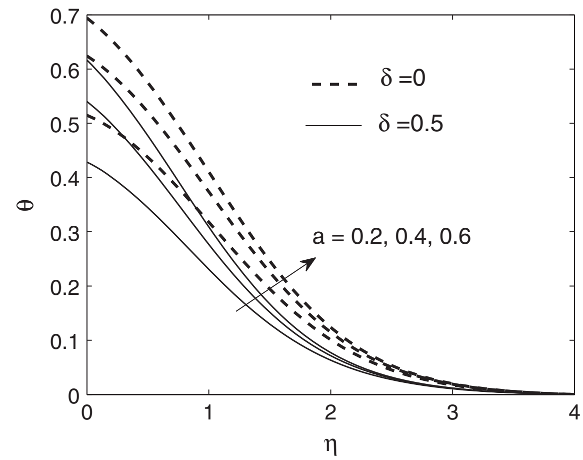

Figure 13 Effects of a and δ on temperature profiles.

For $\theta_r > 0$, it is observed that velocity profiles increase with the increase of θ_r. It is also seen that the change of velocity is negligible for higher values of θ_r because the variable viscosity of the fluid approaches to constant viscosity at ambient temperature. On the other hand, temperature profiles decrease with the increase of positive value of θ_r. That means, increase of variable viscosity parameter makes decrease of thermal boundary layer thickness and results in increase of velocity. The opposite effects can be seen on velocity and temperature profiles for negative values of θ_r. This observation is similar to that of Makinde [48].

Figs. 4 and 5 illustrate effects of temperature ratio parameter (θ_w) on velocity and temperature curves. The thermal state of the fluid is defined by the temperature ratio parameter. The more the temperature ratio parameter means the higher the thermal state of the fluid which increases the temperature as well as velocity profiles of the fluid.

The effects of thermophoretic parameter τ on velocity, temperature and concentration distributions are shown in Figs. 6–8. It is noticed that the temperature of the fluid (Fig. 7) increases whereas the velocity and concentration (Figs. 6 and 8) profiles decrease. Increase of thermophoretic parameter rises the thermophoretic forces which produce the

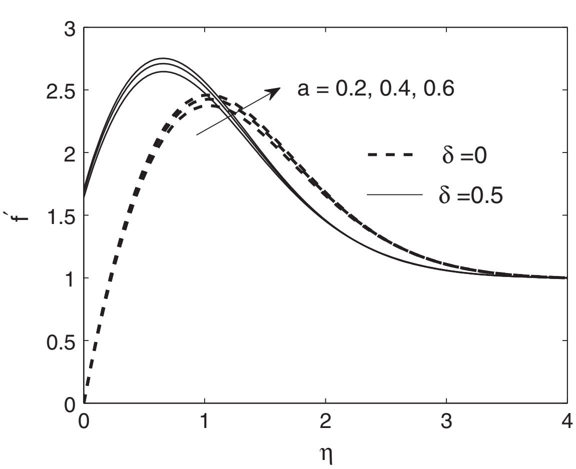

Figure 12 Effects of a and δ on velocity profiles.

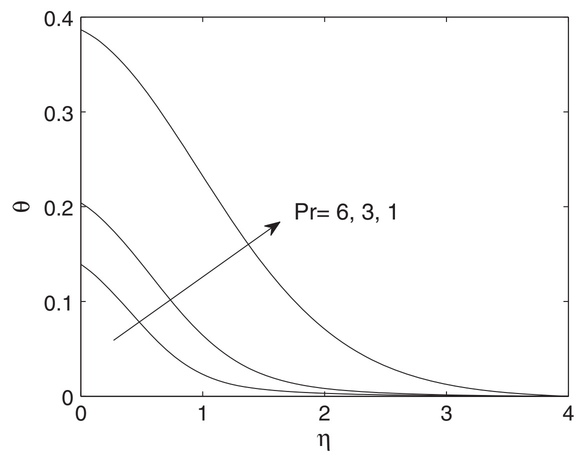

Figure 14 Effects of Prandtl number Pr on temperature profiles.

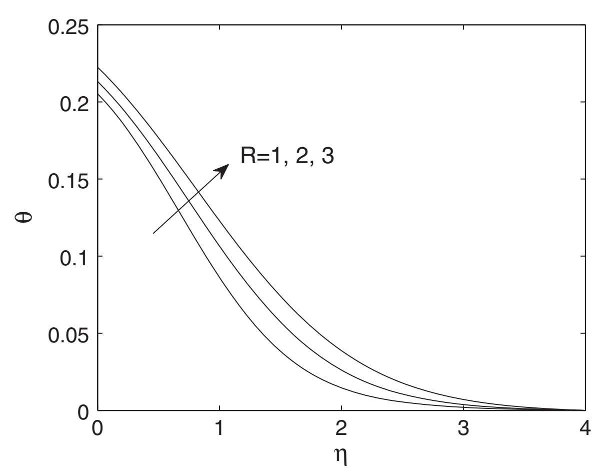

Figure 15 Effects of thermal radiation parameter R on temperature profiles at $Pr = 3$.

thermophoretic velocity in the direction negative to that of temperature gradient. Because of hot wall surface condition the thermophoretic effect leads to less particle flux to the wall

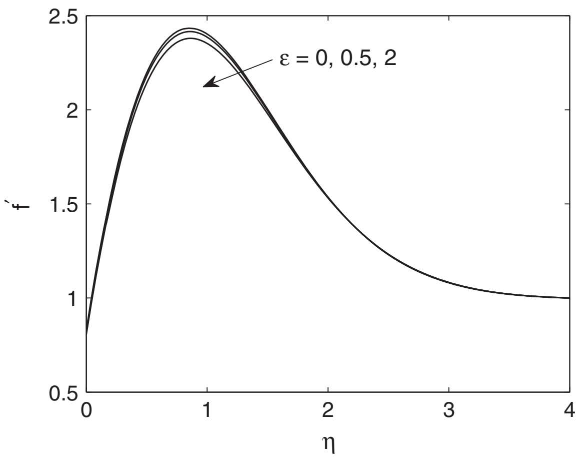

Figure 16 Velocity profiles for various values of thermal conductivity parameter ϵ.

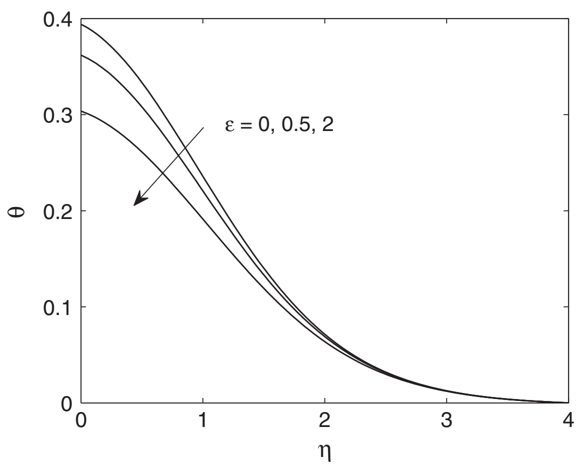

Figure 17 Temperature profiles for various values of thermal conductivity parameter ϵ.

and the particle might be blown away from the surface. Consequently, the concentration decreases with increase in the thermophoretic parameter.

It is observed from Fig. 9 that velocity profiles decrease across the boundary layer with increase of Hartmann number (magnetic parameter) in the absence of slip $\delta = 0$ and in the presence of slip $\delta = 1$. Physically, the higher Lorentz force slows down the motion of the conducting fluid. The additional work used to drag the liquid against magnetic field is dispersed as thermal energy in thermal boundary layer. These outcomes in heating of the boundary layer and therefore the temperature increase in the boundary layer region (Fig. 10). The deceleration of stream because of magnetic force improves the species dispersion in the layer and that outcomes in the increment of concentration (Fig. 11). Further it suggests that the wall slip parameter influences substantially on the flow field parameters.

Figs. 12 and 13 present the velocity and temperature profiles for both slip and no-slip flows. It can be observed from Fig. 13 that the thermal boundary layer increases with the increase in the local surface convection parameter a due to the convective heat exchange between the hot fluid on the

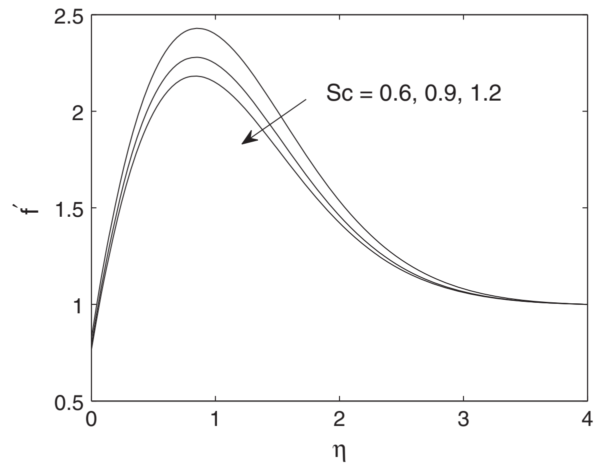

Figure 18 Velocity profiles for various values of Schmidt number Sc.

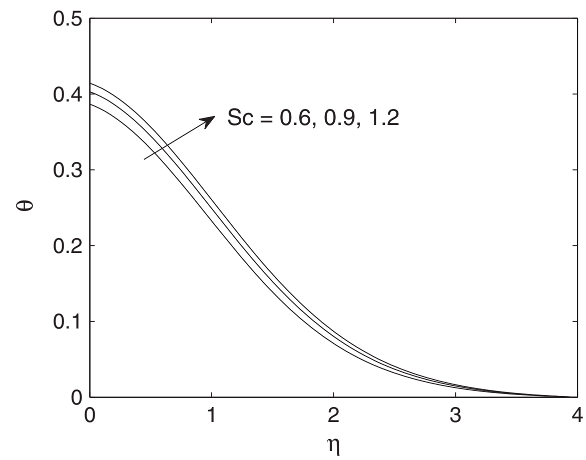

Figure 19 Temperature profiles for various values of Schmidt number Sc.

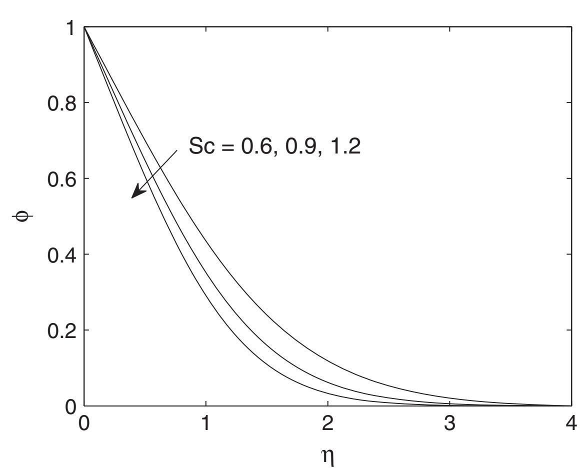

Figure 20 Concentration profiles for various values of Schmidt number Sc.

Table 2 Values of C_f, Nu_x and Sh_x for different values of $R, a, \delta, \epsilon, \theta_r$ and θ_w.

R	a	δ	ϵ	θ_r	θ_w	C_f	Nu_x	Sh_x
0.2	0.1	0.2	0.1	3	1.5	4.4225	0.0785	0.5762
0.4	0.1	0.2	0.1	3	1.5	4.4195	0.0994	0.5788
0.8	0.1	0.2	0.1	3	1.5	4.4100	0.1407	0.5824
0.2	0.3	0.2	0.1	3	1.5	4.8196	0.1868	0.5916
0.2	0.9	0.2	0.1	3	1.5	5.3953	0.3415	0.6121
0.2	0.1	0.5	0.1	3	1.5	3.3070	0.0823	0.6194
0.2	0.1	1.0	0.1	3	1.5	2.3122	0.0850	0.6561
0.2	0.1	0.2	0.5	3	1.5	4.3421	0.0790	0.5743
0.2	0.1	0.2	1.0	3	1.5	4.2653	0.0797	0.5725
0.2	0.1	0.2	0.1	10	1.5	4.1709	0.0803	0.5823
0.2	0.1	0.2	0.1	100	1.5	4.0878	0.0809	0.5843
0.2	0.1	0.2	0.1	∞	1.5	4.0790	0.0810	0.5845
0.2	0.1	0.2	0.1	3	1.0	4.4144	0.0699	0.5750
0.2	0.1	0.2	0.1	3	2.0	4.4366	0.0905	0.5777
0.2	0.1	0.2	0.1	3	3.0	4.4868	0.1273	0.5819

Table 3 Values of C_f, Nu_x and Sh_x for different values of τ, Nc, Sc, Gr and Gc.

τ	Nc	Sc	Gr	Gc	C_f	Nu_x	Sh_x
0.2	0.1	0.6	5	5	4.4225	0.0785	0.5762
0.4	0.1	0.6	5	5	4.4141	0.0784	0.5756
0.8	0.1	0.6	5	5	4.3974	0.0782	0.5747
0.2	0.3	0.6	5	5	4.4210	0.0785	0.5748
0.2	0.9	0.6	5	5	4.4166	0.0784	0.5707
0.2	0.1	0.9	5	5	4.2937	0.0768	0.6825
0.2	0.1	1.2	5	5	4.2016	0.0755	0.7697
0.2	0.1	0.6	10	5	5.1673	0.0823	0.6137
0.2	0.1	0.6	15	5	5.8024	0.0849	0.6432
0.2	0.1	0.6	5	10	6.0873	0.0853	0.6500
0.2	0.1	0.6	5	15	7.6378	0.0894	0.7097

lower side of the plate and the cold fluid on the upper side of the plate. Consequently, velocity profile increases (Fig. 12). The thermal boundary layer made a further reduction in the presence of slip.

The effects of Prandtl number Pr on temperature profiles are shown in Fig. 14. It can be observed that when the Prandtl number is high, the thermal boundary layer thickness is small. Physically, for the high Prandtl number flow the momentum diffusivity dominates the flow. Therefore, the region where thermal diffusion is important becomes smaller. Fig. 15 shows the temperature profiles for various values of radiation parameter. From this result we see that temperature increases with increase of radiation parameter. This result qualitatively agrees well with the fact that the rate of heat transport to the fluid increases with higher values of radiation parameter and thereby the temperature of the fluid increases.

The dimensionless velocity and temperature profiles for different values of variable thermal conductivity parameter ϵ are shown in Figs. 16 and 17. The increase in ϵ means increase of thermal conductivity near the wall and hence the temperature reduces near the wall and the velocity boundary layer also decreases (Fig. 16). It can be further observed that ϵ has negligible effect on temperature far away from the wall.

The variation of Schmidt number (Sc) on velocity, temperature and concentration profiles is shown in Figs. 18–20, respectively. The increase in the value of Sc results in the decrease of velocity and concentration profiles and the reverse effect is observed in case of the temperature profile. Since Schmidt number is the ratio of the viscous diffusion rate to mass diffusion rate, the increase in Sc results in an increase of the viscous diffusion rate which reduces the velocity and hence enhances the temperature in the fluid.

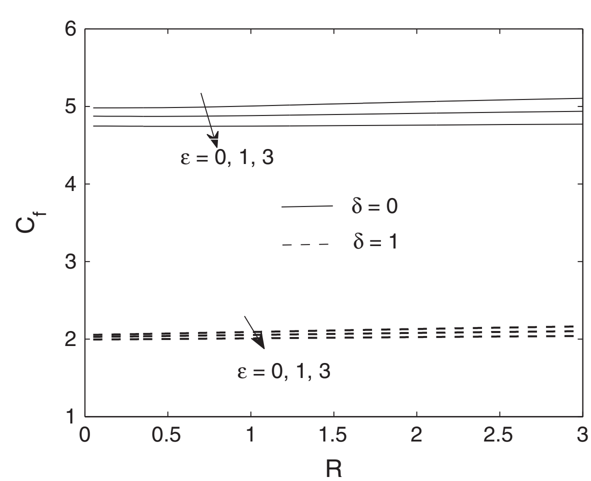

Figure 21 C_f vs. R effect of ϵ and δ.

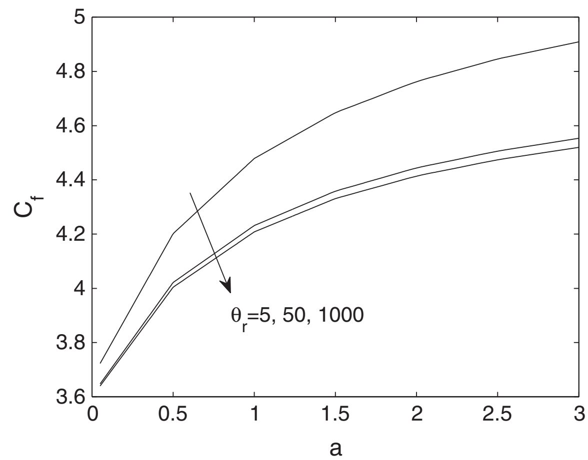

Figure 22 C_f vs. a effect of θ_r.

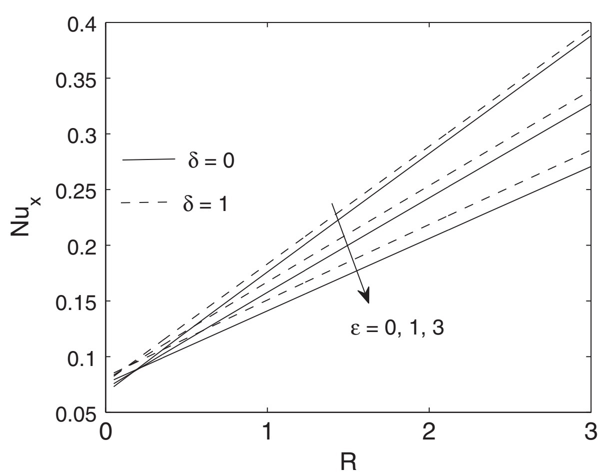

Figure 23 Nu_x vs. R effects of ϵ and δ.

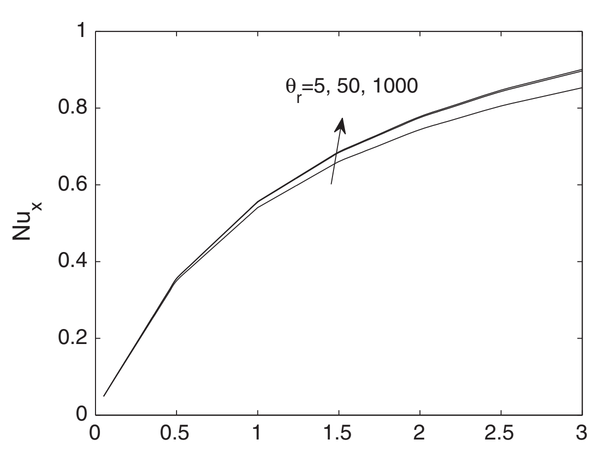

Figure 24 Nu_x vs. a effect of θ_r.

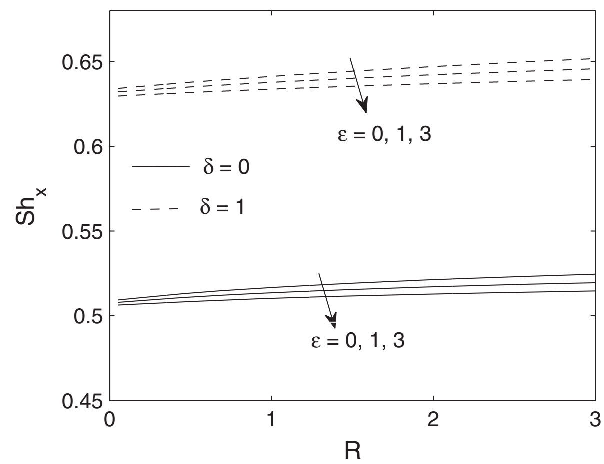

Figure 25 Sh_x vs. R and effects ϵ and δ.

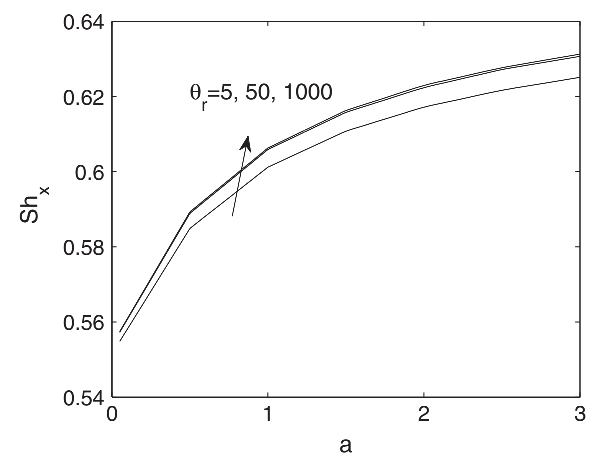

Figure 26 Sh_x vs. a effect of θ_r.

3.3. Computational results for coefficient of skin friction, Nusselt number and Sherwood number

For validating the accuracy of our numerical results, we have compared our results with the previous published data from Rahman [6] in Table 1. Results for ambient Prandtl number at the surface of the plate versus different values of fluid viscosity parameter θ_r and slip parameter δ compared with those of Rahman [6] when $Q_s = Q_t = 0, R = 0, \epsilon = 0.5, a = 0.5, Pr = 1.0, Ha = 1.0$ and in the absence of mass transfer. It can be seen that the comparison in all cases is found to be in good agreement.

Tables 2 and 3 show the calculated values of skin friction, Nusselt number and Sherwood number for various values of fluid parameters. It can be noted that the skin friction, Nusselt number and Sherwood number increase whenever there is an increase in the value of Gr, GC, a and θ_w. From these tables it is observed that the radiation parameter R, slip parameter δ, and variable viscosity parameter θ_r reduces the shear stress whereas the reverse effect occurs for the rate of heat and mass transfer. It can be further noted that the skin friction, Nusselt number and Sherwood number decrease with the increase of thermophoretic parameter and concentration difference parameter. Further the mass transfer rate is considerably higher for higher value of Schmidt number.

A graphical representation of the variation of skin friction (C_f) with the radiation parameter R is given in Fig. 21 for various values of variable thermal conductivity parameter (ϵ) and slip parameter (δ). The presence of slip condition ($\delta = 1$) permits the fluid to slip past the sheet and the skin friction coefficient decreases and causes the increase of rate of heat and mass transfer (Figs. 23 and 25). It is further observed that the fluid with high variable thermal conductivity parameter promotes conduction and thereby reduce the shear stress and the rate of heat and mass transfer. The increase of radiation parameter increases the heat flux near the plate, which increases the heat transfer rate (Fig. 23) and also the value of the local Sherwood number. In Fig. 22 we plot skin friction versus surface convection parameter (a) for various values of variable viscosity parameter θ_r. This result shows that the skin friction increases with surface convection parameter (a), but decreases with θ_r. The temperature at the plate increases with the increase of surface convection parameter and hence it enhances the rate of heat transfer (Fig. 24) and increase in the mass transfer rate (Fig. 26).

4. Summary and conclusions

The effects of thermal radiation, thermophoresis, variable viscosity and variable thermal diffusivity on steady heat and mass transfer process in a two-dimensional MHD convective flow over a flat plate with partial slip at the surface were studied numerically. The radiative heat flux is modeled through the non-linear Rosseland diffusion approximation, which produces one new temperature ratio parameter. The present study reveals that this parameter influences velocity and temperature fields significantly. The variable thermodynamic transport coefficients provide strong coupling among energy, mass and momentum equations. The effects of various physical parameters on fluid flow, heat and mass transfer phenomena have been studied. Finally we arrived at the following major findings:

- The temperature profile and the rate of heat transfer at the wall reduce as the variable thermal conductivity parameter rises.
- The velocity and temperature distribution will rise having higher value of the temperature ratio parameter while the opposite effect is observed in the case of thermal conductivity parameter.
- The temperature profiles are higher for the case of no-slip than for the presence of slip.
- In the presence of magnetic field the velocity profile decreases with increasing induction drag. On the other hand, it enhances the temperature and concentration.
- The Prandtl number controls the thermal boundary layer. An increasing Prandtl number causes decrease in the thermal boundary layer.
- The rate of heat transfer to the fluid increases with increase in radiation parameter.
- The species concentration decreases with the increase of thermophoretic parameter and Schmidt number.
- The local skin friction, Nusselt number and Sherwood number increase with the increase in Grashof number, solutal Grashof number and the surface convection parameter.
- The wall stress decreases with the presence of slip and the Nusselt and Sherwood numbers increase.

These results have possible technological applications such as fabrication of optical fiber and nuclear reactor and are expected to be very useful for practical applications.

Acknowledgment

We thank the reviewers for their valuable comments and suggestions that have substantially improved our manuscript.

References

[1] H. Blasius, Grenzschichten in Flüssigkeiten mit kleiner Reibung, Inaugural-Dissertation, von H. Blasius, Druck von BG Teubner, 1907.

[2] T. Fang, Similarity solutions for a moving-flat plate thermal boundary layer, Acta Mech. 163 (3–4) (2003) 161–172.

[3] O.D. Makinde, Free convection flow with thermal radiation and mass transfer past a moving vertical porous plate, Int. Commun. Heat Mass Transfer 32 (10) (2005) 1411–1419.

[4] R. Cortell, Numerical solutions of the classical Blasius flat-plate problem, Appl. Math. Comput. 170 (1) (2005) 706–710.

[5] J.J. Shu, I. Pop, On thermal boundary layers on a flat plate subjected to a variable heat flux, Int. J. Heat Fluid Flow 19 (1) (1998) 79–84.

[6] M.M. Rahman, Locally similar solutions for hydromagnetic and thermal slip flow boundary layers over a flat plate with variable fluid properties and convective surface boundary condition, Meccanica 46 (5) (2011) 1127–1143.

[7] A. Aziz, A similarity solution for laminar thermal boundary layer over a flat plate with a convective surface boundary condition, Commun. Nonlinear Sci. Numer. Simul. 14 (4) (2009) 1064–1068.

[8] R.C. Bataller, Radiation effects for the Blasius and Sakiadis flows with a convective surface boundary condition, Appl. Math. Comput. 206 (2) (2008) 832–840.

[9] A. Ishak, Similarity solutions for flow and heat transfer over a permeable surface with convective boundary condition, Appl. Math. Comput. 217 (2) (2010) 837–842.

[10] S. Yao, T. Fang, Y. Zhong, Heat transfer of a generalized stretching/shrinking wall problem with convective boundary conditions, Commun. Nonlinear Sci. Numer. Simul. 16 (2) (2011) 752–760.

[11] M.J. Uddin, O.A. Beg, A. Aziz, A.I. Md. Ismail, Group analysis of free convection flow of a magnetic nanofluid with chemical reaction, Math. Prob. Eng. (2015). Article ID 621505, <http://dx.doi.org/10.1155/2015/621503>.

[12] M.J. Uddin, W.A. Khan, A.I. Md. Ismail, Scaling group transformation for MHD boundary layer slip flow of a nanofluid over a convectively heated stretching sheet with heat generation, Math. Prob. Eng. (2012). Article ID 934964, <http://dx.doi.org/10.1155/2012/934964>.

[13] M.J. Uddin, M. Ferdows, O.A. Beg, Group analysis and numerical computation of magneto-convective non-Newtonian nanofluid slip flow from a permeable stretching sheet, Appl. Nanosci. 4 (2014) 897–910.

[14] M.J. Uddin, O.A. Beg, N. Amin, Hydromagnetic transport phenomena from a stretching or shrinking nonlinear nanomaterial sheet with Navier slip and convective heating: a model for bio-nano-materials processing, J. Magn. Magn. Mater. 368 (2014) 252–261.

[15] K.V. Prasad, K. Vajravelu, Heat transfer in the MHD flow of a power law fluid over a non-isothermal stretching sheet, Int. J. Heat Mass Transfer 52 (21) (2009) 4956–4965.

[16] M. Subhas Abel, P.G. Siddheshwar, N. Mahesha, Effects of thermal buoyancy and variable thermal conductivity on the MHD flow and heat transfer in a power-law fluid past a vertical stretching sheet in the presence of a non-uniform heat source, Int. J. Non-Linear Mech. 44 (1) (2009) 1–12.

[17] E.M.E. Elbarbary, N.S. Elgazery, Flow and heat transfer of a micro polar fluid in an axisymmetric stagnation flow on a cylinder with variable properties and suction (numerical study), Acta Mech. 176 (3–4) (2005) 213–229.

[18] M.A. Seddeek, A.M. Salem, The effect of an axial magnetic field on the flow and heat transfer about a fluid underlying the axisymmetric spreading surface with temperature dependent viscosity and thermal diffusivity, Comput. Mech. 39 (4) (2007) 401–408.

[19] Mohammad M. Rahman, K.M. Salahuddin, Study of hydromagnetic heat and mass transfer flow over an inclined heated surface with variable viscosity and electric conductivity, Commun. Nonlinear Sci. Numer. Simul. 15 (8) (2010) 2073–2085.

[20] I.J. Rao, K.R. Rajagopal, The effect of the slip boundary condition on the flow of fluids in a channel, Acta Mech. 135 (3–4) (1999) 113–126.

[21] Ann Yoshimura, Robert K. Prud'homme, Wall slip corrections for Couette and parallel disk viscometers, J. Rheol. 32 (1) (1988) 53–67.

[22] H. Hasimoto, Boundary layers slip condition for a flat plate, J. Aeronaut. Soc. 25 (1958) 68–69.

[23] M.J. Martin, I.D. Boyd, Blasius Boundary Layer Solution with Slip Flow Conditions, The American Institute of Physics, 2001.

[24] M.J. Martin, I.D. Boyd, Momentum and heat transfer in laminar boundary layer with slip flow conditions, J. Thermophys. Heat Transfer 20 (2006) 710–719.

[25] M.J. Martin, I.D. Boyd, Falkner-Skan flow over a wedge with slip boundary conditions, J. Thermophys. Heat Transfer 24 (2) (2010) 263–270.

[26] N.K. Vedantam, R.N. Parthasarathy, Effects of slip on the flow characteristics of laminar flat plate boundary-layer, in: ASME 2006 2nd Joint US-European Fluids Engineering Summer Meeting Collocated With the 14th International Conference on Nuclear Engineering, 2006, pp. 1551–1560.

[27] T. Fang, Chia-fon F. Lee, A moving-wall boundary layer flow of a slightly rarefied gas free stream over a moving flat plate, Appl. Math. Lett. 18 (5) (2005) 487–495.

[28] H.I. Andersson, Slip flow past a stretching surface, Acta Mech. 158 (1–2) (2002) 121–125.

[29] C.Y. Wang, Analysis of viscous flow due to a stretching sheet with surface slip and suction, Nonlinear Anal.: Real World Appl. 10 (1) (2009) 375–380.

[30] A. Aziz, Hydrodynamic and thermal slip flow boundary layers over a flat plate with constant heat flux boundary condition, Commun. Nonlinear Sci. Numer. Simul. 15 (3) (2010) 573–580.

[31] B. Sahoo, Flow and heat transfer of a non-Newtonian fluid past a stretching sheet with partial slip, Commun. Nonlinear Sci. Numer. Simul. 15 (3) (2010) 602–615.

[32] M.A. Seddeek, A.A. Darwish, M.S. Abdelmeguid, Effects of chemical reaction and variable viscosity on hydromagnetic mixed convection heat and mass transfer for Hiemenz flow through porous media with radiation, Commun. Nonlinear Sci. Numer. Simul. 12 (2) (2007) 195–213.

[33] D. Pal, B. Talukdar, Perturbation analysis of unsteady magnetohydrodynamic convective heat and mass transfer in a boundary layer slip flow past a vertical permeable plate with thermal radiation and chemical reaction, Commun. Nonlinear Sci. Numer. Simul. 15 (7) (2010) 1813–1830.

[34] A. Mahdy, Effect of chemical reaction and heat generation or absorption on double-diffusive convection from a vertical truncated cone in porous media with variable viscosity, Int. Commun. Heat Mass Transfer 37 (5) (2010) 548–554.

[35] B.R. Rout, S.K. Parida, S. Panda, MHD heat and mass transfer of chemical reaction fluid flow over a moving vertical plate in presence of heat source with convective surface boundary condition, Int. J. Chem. Eng. (2013), http://dx.doi.org/10.1155/2013/296834.

[36] C.S. Balla, K. Naikoti, Radiation effects on unsteady MHD convective heat and mass transfer past a vertical plate with chemical reaction and viscous dissipation, Alexand. Eng. J. Online (2015), <http://www.sciencedirect.com/science/article/pii/S111001681500071X>.

[37] M.M. Rahman, A. Aziz, M.A. Al-Lawatia, Heat transfer in micro polar fluid along an inclined permeable plate with variable fluid properties, Int. J. Therm. Sci. 49 (6) (2010) 993–1002.

[38] M.M. Rahman, M.A. Rahman, M.A. Samad, M.S. Alam, Heat transfer in a micro polar fluid along a non-linear stretching sheet with a temperature-dependent viscosity and variable surface temperature, Int. J. Thermophys. 30 (5) (2009) 1649–1670.

[39] R. Cortell, Fluid flow and radiative nonlinear heat transfer over a stretching sheet, J. King Saud Univ. – Sci. 26 (2014) 161–167.

[40] P. Goldsmith, F.G. May, Diffusiophoresis and thermophoresis in water vapour systems, in: Aerosol Science, Academic Press, London, 1966, pp. 163–194.

[41] M.S. Alam, M.M. Rahman, M.A. Sattar, Effects of variable suction and thermophoresis on steady MHD combined free-forced convective heat and mass transfer flow over a semi-infinite permeable inclined plate in the presence of thermal radiation, Int. J. Therm. Sci. 47 (6) (2008) 758–765.

[42] M.F. El-Sayed, N.S. Elgazery, Effect of variations in viscosity and thermal diffusivity on MHD heat and mass transfer flow over a porous inclined radiate plane, Eur. Phys. J. Plus 126 (12) (2011) 1–16.

[43] K. Das, S. Jana, P.K. Kundu, Thermophoretic MHD slip flow over a permeable surface with variable fluid properties, Alexand. Eng. J. 54 (2015) 35–44.

[44] T.C. Chiam, Heat transfer with variable conductivity in a stagnation-point flow towards a stretching sheet, Int. Commun. Heat Mass Transfer 23 (2) (1996) 239–248.

[45] E.M. Sparrow, R.D. Cess, Radiation Heat Transfer (Series in Thermal and Fluids Engineering), Harpercollins College Div, 1978, ISBN 10: 0070599106, ISBN 13: 9780070599109.

[46] L. Talbot, R.K. Cheng, R.W. Schefer, D.R. Willis, Thermophoresis of particles in a heated boundary layer, J. Fluid Mech. 101 (04) (1980) 737–758.

[47] G.K. Batchelor, C. Shen, Thermophoretic deposition of particles in gas flowing over cold surfaces, J. Colloid Interface Sci. 107 (1) (1985) 21–37.

[48] O.D. Makinde, Effect of variable viscosity on thermal boundary layer over a permeable flat plate with radiation and a convective surface boundary condition, J. Mech., Sci. Technol. 26 (5) (2012) 1615–1622.